Benchmarking EGSnrc in the kilovoltage energy range against experimental measurements of charged particle backscatter coefficients

E S M Ali and D W O Rogers

Carleton Laboratory for Radiotherapy Physics, Ottawa Carleton Institute of Physics,
Carleton University, 1125 Colonel By Drive, Ottawa, ON K1S 5B6, Canada

E-mail: eali@physics.carleton.ca and drogers@physics.carleton.ca

Abstract

This study benchmarks the EGSnrc Monte Carlo code in the energy range of interest to kilovoltage medical physics applications (5–140 keV) against experimental measurements of charged particle backscatter coefficients. The benchmark consists of experimental data from 20 different published experiments (1954–2007) covering 35 different elements ($4 \leqslant Z \leqslant 92$), electron and positron backscatter, normal and oblique incidence, and backscatter from thin films. EGSnrc simulation results show excellent agreement with the vast majority of the experimental data. Possible experimental and computational uncertainties explaining the few noted discrepancies are discussed. This study concludes that for the energy range of interest to kilovoltage medical physics application, EGSnrc produces backscatter results within ∼4% of the average of the majority of published experimental data. A documented EGSnrc user-code customized for backscatter calculations is available from the authors at http://www.physics.carleton.ca/clrp/backscatter.

(Some figures in this article are in colour only in the electronic version)

1. Introduction

Accurate characterization of charged particles (electrons and positrons) backscattered from solid surfaces is important to many kilovoltage medical physics applications. Such applications include predicting dose perturbations due to high-Z inhomogeneities in tissue (Verhaegen 2002, Buffa and Verhaegen 2004), studying the performance of an x-ray tube when placed in the magnetic field of an MR scanner in hybrid CT/MRI systems (Wen *et al* 2007a, 2007b), and quantifying the effect of off-focal radiation on the output of

x-ray systems (Ali and Rogers 2008b). However, accurate charged particle backscatter simulations are one of the most challenging tasks for any Monte Carlo radiation transport code that uses the condensed history technique (Kawrakow 2000). Thus, rigorous testing of Monte Carlo codes is needed before their generated backscatter data are deemed accurate.

In recent year, there has been a growing interest in using the EGSnrc Monte Carlo code (Kawrakow 2000, Kawrakow and Rogers 2007) for kilovoltage medical physics applications (Verhaegen and Castellano 2002, Ebert and Carruthers 2003, Buffa and Verhaegen 2004, Agyingi *et al* 2005, Azner *et al* 2005, Verhaegen *et al* 2005, Zeng and McCaffrey 2005, Deloar *et al* 2006, Jarry *et al* 2006, La Russa and Rogers 2006, Mainegra-Hing and Kawrakow 2006, Taylor *et al* 2006, Ali and Rogers 2007, Bazalova and Verhaegen 2007, Ding *et al* 2007, Hill *et al* 2007, La Russa *et al* 2007, Ali and Rogers 2008b, Chow *et al* 2008). This steady increase can be attributed to the accurate low-energy physics in the code, the multitude of variance reduction techniques available in EGSnrc and its user-codes, the code's adoption of the most accurate photon and charged-particle cross sections available (Seltzer and Berger 1985, Seltzer and Berger 1986, Berger and Hubbell 1987), the increasing clinical trend of integrating kilovoltage imaging units with most therapy systems, and finally, the increase in computing power per unit cost which makes Monte Carlo more appealing than ever. This places a strong need for diverse testing of EGSnrc in the kilovoltage range. This study aims at fulfilling this need for the energy range of interest to kilovoltage medical physics applications (5–140 keV).

The few published EGSnrc benchmarks in the kilovoltage range are mostly subsets of larger studies that focus more on the megavoltage range (^{60}Co and above), or have a split focus at best. In this paragraph, the kilovoltage parts of these studies are highlighted. Kawrakow (2000) showed that for 10 and 100 keV electron beams normally incident on a semi-infinite water phantom, the fraction of energy reflected, i.e. backscattered, calculated using the EGSnrc condensed history algorithm, is step-size independent and that it agrees within 0.1% with single scattering calculations. Borg *et al* (2000) tested EGSnrc against NRC experimental measurements of relative ion-chamber response versus beam quality for kilovoltage photon beams. They showed agreement within 0.5% for tube potentials of 50–250 kVp. The agreement was within 3% for lower kVps due to uncertainties in ion-chamber impurity levels and geometrical details. Kawrakow and Rogers (2001) compared EGSnrc calculations of electron backscatter coefficients to experimental data and showed that including electron spin in EGSnrc simulations is essential to get better agreement with experimental data. However, the study was done for aluminium and gold only, and with very few experimental datasets per element. In addition, oblique incidence, thin films and positron backscatter were not investigated. Verhaegen (2002) reported good agreement between EGSnrc simulation results and parallel-plate ion-chamber measurements of interface perturbations in kilovoltage photon beams. Most recently, Mainegra-Hing and Kawrakow (2006) showed agreement within 2% between EGSnrc simulation results and NRC experimental measurements of half value layers for an x-ray tube operating in the range 120–200 kVp.

The charged particle backscatter coefficient (η) is defined as the probability that a charged particle incident on a semi-infinite sample backscatters into the hemisphere above the sample. By definition, η does *not* include electrons from *secondary electron emission* which is the generation of very low-energy surface electrons (conventionally with kinetic energy <50 eV). This study examines the capability of EGSnrc to accurately predict η for incident charged particles with kinetic energy in the kilovoltage range. The benchmark consists of experimental data from 20 different published experiments covering 35 different elements ($4 \leqslant Z \leqslant 92$),

electron and positron backscatter, normal and oblique incidence, and backscatter from thin films. A related study comparing EGSnrc simulation results with experimental measurements for the energy spectra and angular distributions of backscattered charged particles has been published elsewhere (Ali and Rogers 2008a).

2. Methods

2.1. Experimental measurements

The 20 experiments included in this benchmark are all the experiments in the literature that were reported after 1950 (Bishop 1965, Coleman *et al* 1992, Coslett and Thomas 1965, Drescher *et al* 1970, Fitting and Technow 1983, Heinrich 1965, Hunger and Küchler 1979, Kulenkampff and Spyra 1954, Mäkinen *et al* 1992, Martin *et al* 2006, Massoumi *et al* 1991, Massoumi *et al* 1993, Neubert and Rogaschewski 1980, Niedrig 1982, Niedrig and Sieber 1971, Radzimski 1978, Soum *et al* 1984, Weinryb and Philibert 1964, Wittry 1965, Yadav and Shanker 2007). No emphasis is put on a particular experiment, and the data from all experiments are assumed to be equally valid. All experimental data are taken from their original sources, except those by Niedrig (1982) which he reproduced from a PhD thesis. When experimental data are not available in tabular form, they are digitized electronically from their original graphs. The experimental data by Coleman *et al* (1992) and Martin *et al* (2006) are newer versions of previous measurements by the same investigators— Baker and Coleman (1988) and Martin *et al* (2003), respectively—and only the newer data are included in this study. Additional notes on specific experiments are mentioned in section 3.

In a typical electron backscatter experiment, electrons of a known energy impinge onto a polished sample at a specific angle. The experiment operates at low pressure ($\sim 10^{-4}$ torr) to reduce sample contamination and electron scatter. Backscattered electrons are collected using a hemispherical collecting electrode and the backscatter current is measured. The backscatter coefficient (η) as defined in section 1 is then the ratio of the backscattered current to the incident current. Some experiments use a small detector instead of the hemispherical collector. In this case, a series of measurements are made at different detector angles to determine the differential backscatter coefficient with respect to the detector angle, then numerical integration is used to estimate the overall η. Experiments suppress secondary electron emission (discussed in section 1) by either biasing the sample at +50 V to prevent secondary electrons from escaping the sample, or by surrounding the sample with a perforated retarding grid typically biased at -50 V to prevent secondary electrons from reaching the collecting electrode or the detector. The value of ± 50 V for the bias is typically used because it has been observed experimentally (Heinrich 1965, Wittry 1965) that when the absolute value of the bias is incrementally changed from 50 V to a few hundred volts, the backscatter current does not change. Retarding grids, however, have the disadvantage that they require correction factors to account for their intercepting a fraction of the true backscattered electrons and preventing them from reaching the collecting electrode or detector. In positron backscatter experiments, the backscatter is indirectly estimated from measurements of the annihilation count rate of positrons decaying in the sample, i.e. those that did *not* backscatter. For more details on the experimental setups, the reader is referred to the original articles of the electron and positron backscatter experiments listed above.

Although measurements of charged particle backscatter coefficients are conceptually simple, they are very challenging in practice, and they are fraught with many sources of uncertainty. Knowledge of these uncertainties is essential for meaningful comparison between
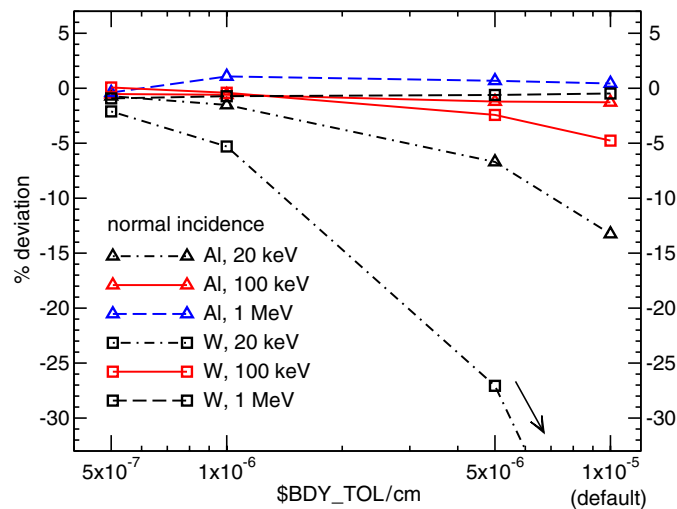
experimental data and EGSnrc simulation results. The following is a summary of a few of those uncertainties. Secondary electron emission causes over-estimation of η_- if not properly eliminated. Retarding grids cause under-estimation of η_- if their presence is not corrected for. Even when correction factors are used for retarding grids, there are non-negligible uncertainties associated with these correction factors (Bishop 1965). Small differences in the experimental setup or operational parameters can have a considerable effect on the low-energy electron currents (Heinrich 1965). Voltage bias details can cause backscattered electrons to re-impinge on the sample, i.e. not contribute to the backscatter current and hence η_- is under-estimated, or to generate electrons from parts of the experimental setup other than the sample (Heinrich 1965), i.e. η_- is over-estimated. Sample contamination, which can be reduced (but not eliminated) by cleaning and polishing the sample surface and by operating at low pressure, leads to under-estimation of η_- because surface contaminants are generally lower-Z materials with lower backscatter coefficient than the sample material. Surface contamination is more important at lower energies and at near-grazing incidence (Coleman *et al* 1992) because the effective perpendicular penetration of the charged particle decreases, which enhances the effect of the contaminant layer. Uncertainty in the thickness of film samples can be up to 10% (Rau *et al* 2002). Setup constraints can lead to deviations of up to $5°$ from normal incidence while still calling it normal incidence (Coleman *et al* 1992, Mäkinen *et al* 1992). At near-grazing incidence angles, the non-zero diameter of the incident beam can become an issue because it becomes harder to guarantee that all incident charged particles hit the sample (Massoumi *et al* 1993). Similarly, at near-grazing backscatter angles, and because of the finite solid angle subtended by the detector, a portion of the detector may be masked by the sample itself which leads to under-estimation of η (Massoumi *et al* 1991). Electrons backscattered from the sample may backscatter again at the face of the detector, or they may completely stop in the detector entrance window (Massoumi *et al* 1993, Gérard *et al* 1995). This effect may cancel out because it affects the measurement of both the incident and the backscattered current, assuming the effect is energy independent. For the experiments discussed above that use small detectors rather than hemispherical collectors, the uncertainties associated with their techniques can be $\sim$10% for $Z > 20$, and $>$10% for $Z < 20$ (Massoumi *et al* 1993). For positron backscatter measurements, the uncertainty associated with the annihilation technique discussed earlier is that energetic positrons backscattered at a large angle may annihilate in front of the detector and get recorded as if they occurred in the sample. This causes under-estimation of η_+ which gets worse as the kinetic energy of the incident positrons increases (Coleman *et al* 1992). For more details on the uncertainties associated with each experiment, the reader is referred to the original articles of the individual experiments.

Some of the uncertainties discussed above are more challenging than others, and some experiments are more careful than others in reducing them. One of the most recent experiments included in this study (Martin *et al* 2006) used two different measurement techniques: current integration and silicon detector measurements, with reported reproducibility of 5% and 7%, respectively. With the addition of other uncertainties, the reported overall uncertainty is 9% and 12%, respectively. In general for experiments measuring charged particle backscatter, the overall uncertainty is higher for lower incident charged particle energies (due to low-energy electron currents, sample contamination, detector entrance window, etc), and for lower-Z samples (due to smaller backscatter yield). The uncertainties discussed above can explain the variation between different experiments measuring the same parameter. They can also help in evaluating the quality of agreement between EGSnrc simulation results and the experimental data.

2.2. EGSnrc simulations

Simulations are done using DOSRZnrc (Rogers *et al* 2000), an EGSnrc user-code. Many other user-codes could be used instead of DOSRZnrc and the same results would be obtained except that when BEAMnrc (Rogers *et al* 1995, Rogers *et al* 2007) is used, an adjustment to one of its internal parameters has to be made in order to get accurate kilovoltage backscatter data—see below. Simulations include a pencil beam of monoenergetic charged particles ($5 \leqslant E_0 \leqslant 140$ keV) incident on a sample ($4 \leqslant Z \leqslant 92$) with a thickness larger than the range of the charged particles in the sample material, except when thin film samples are simulated. The most accurate low-energy physics (Kawrakow and Rogers 2007) and cross-section data (Seltzer and Berger 1985, Seltzer and Berger 1986, Berger and Hubbell 1987) available in EGSnrc are employed. Backscattered charged particles are tallied as they cross from the sample medium back to the vacuum. The values of AE, AP, ECUT and PCUT (Kawrakow and Rogers 2007) used in the simulations are 512, 1, 512 and 1 keV, respectively.

Our sensitivity analysis shows that the calculations of η are insensitive to the exact choice of AP and PCUT because backscattered electrons that are created by photons have a minor contribution to η. Even if photons are immediately discarded, they introduce no more than 1% systematic uncertainty in the value of η. For electrons, the values of AE and ECUT used in this study correspond to a kinetic energy of 1 keV, which is higher than the 50 eV cut-off in the definition of η (section 1) and in the experimental setups (section 2.1). The effect of backscattered electrons with kinetic energy between 50 eV and 1 keV on the value of η in both the experiments and the simulations is investigated. For experiments, as discussed in section 2.1, no change was observed in the backscatter current when the absolute value of the retarding grid bias was changed from 50 V to a few hundred volts—although no experiment tested a bias as high as 1 keV. This indicates that the contribution of very low-energy backscattered electrons is negligible. Additionally, the experimental energy spectra of backscattered electrons approach zero at very low values of the energy of backscattered electrons (Ali and Rogers 2008a). For simulations, the limitations of EGSnrc at very low energies are investigated. EGSnrc uses stopping power values (ICRU 1984) that are based on the Bethe–Bloch theory (Bethe 1930, 1932, Bloch 1933) which assumes that the electron kinetic energy is much larger than the mean ionization energy, I. A kinetic energy of 10 keV is a commonly-accepted lower limit for the applicability of the theory (ICRU 1984), but the theory is known to be sufficiently accurate down to ~1 keV. Below 1 keV, the theory substantially under-estimates the stopping power compared to more sophisticated low-energy models. For instance, the stopping power estimated using the Bethe–Bloch theory becomes negative below 0.15 keV and 0.7 keV for aluminium and gold, respectively—see figure 8.5 in ICRU (1984). In EGSnrc, in addition to the inaccurate stopping power values below 1 keV, there is a lack of energy loss straggling for sub-1 keV interactions, and the cross section data is not available for elastic scattering, electron impact ionization and other processes. Despite knowing the limitations, a few calculations tracking electrons down to below 1 keV are performed, and $\leqslant$2% increase in η is observed compared to calculations down to only 1 keV. However, because the stopping power used in EGSnrc in the range 50 eV–1 keV is less than it should be, more backscattered electrons are simulated in that energy range than should be. The experimental and simulation observations discussed above indicate that 2% is a conservative estimate of the systematic uncertainty introduced in EGSnrc simulations when using an electron kinetic energy cut-off of 1 keV instead of 50 eV for η calculations. Combining the systematic uncertainties due to energy cut-offs for photons and electrons, the overall systematic uncertainty in EGSnrc simulations is $\leqslant$3% which constitutes a limitation of our analysis. However, as will be seen in section 3,

Figure 1. Effect of the boundary tolerance parameter ($BDY_TOL) on the accuracy of backscatter coefficient calculations in aluminium and tungsten using BEAMnrc. The correct values are determined using DOSRZnrc which does not use the $BDY_TOL parameter. The arrow goes to -50% at the default value of $BDY_TOL. The scale of the abscissa is logarithmic.

EGSnrc simulation results remain well within the scatter of the experimental data. In addition to the $\leqslant 3\%$ systematic uncertainty, the statistical uncertainty is $<0.1\%$ which can be achieved within a few minutes of CPU time on a single 3.0 GHz Intel-$^{®}$ Woodcrest 64-bit processor.

When η was evaluated using BEAMnrc instead of DOSRZnrc—in the context of studying off-focal radiation in x-ray systems (Ali and Rogers 2008b)—the results were sensitive to the choice of the *boundary tolerance*, one of the internal parameters of BEAMnrc. This parameter is used to avoid round-off errors by artificially moving the boundaries between different regions in the geometry by a small distance, $BDY_TOL. User-codes other than BEAMnrc use a different technique to avoid round-off errors. Since 2005, the default value of $BDY_TOL has been 10^{-5} cm, and the user has the option to adjust it. This very small boundary adjustment has no effect in the megavoltage range where BEAMnrc is used most often. However, it is too large for kilovoltage applications because the charged particle step size is of the same order of magnitude. This affects backscatter coefficient calculations because the backscattered electrons cross the boundary from the vacuum to the sample material then cross it back to the vacuum. Figure 1 shows the variation with $BDY_TOL of the per cent deviation of BEAMnrc results from the correct value of the total backscatter coefficient as determined by DOSRZnrc for low- and high-Z samples in three different energy ranges. The default value of $BDY_TOL is adequate at megavoltage energies regardless of the atomic number of the target material. At about 100 keV, the default value can cause deviations of up to 5% for high-Z targets. In the mammography range with a high-Z target, the deviation can be up to 50%. In addition, the default value of $BDY_TOL causes a slight shift in the energy spectrum of the backscattered electrons towards lower values (not shown). When $BDY_TOL is reduced to 5×10^{-7} cm, deviations in the total backscatter coefficient are limited to less than 2% for the extreme case of a mammography system. Thus, to simulate x-ray tubes accurately using BEAMnrc, particularly when electron backscatter is the focus, it is essential to use this smaller value of $BDY_TOL. Values of $BDY_TOL lower than 5×10^{-7} cm require BEAMnrc to run fully in double precision.
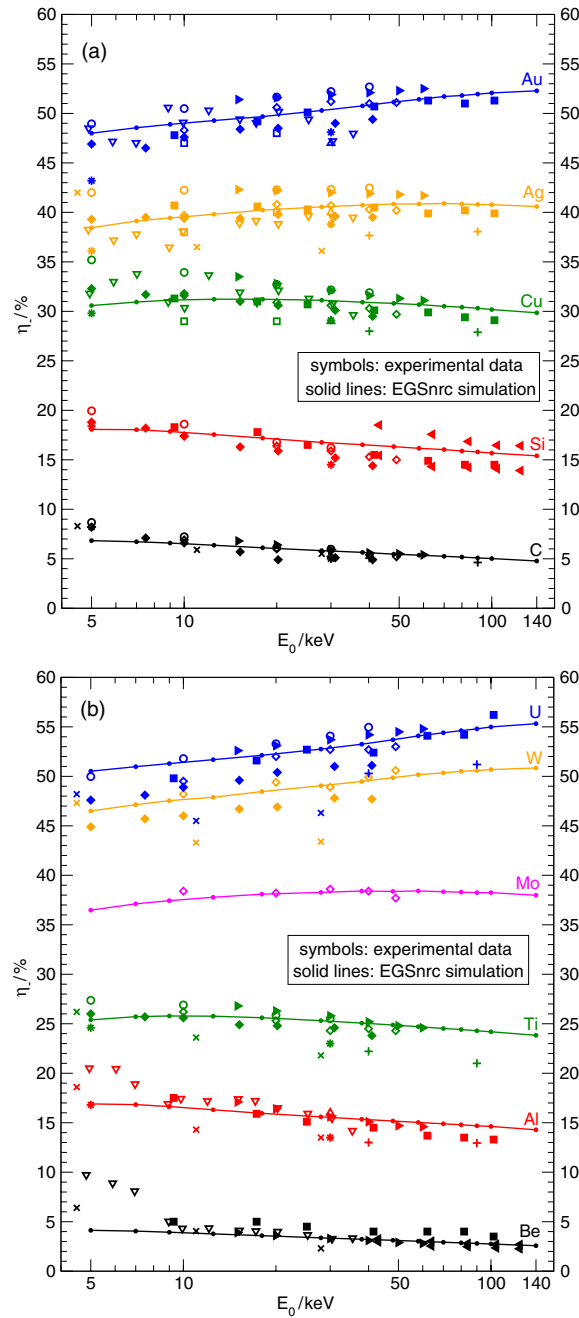
3. Results and discussion

In this section, comparisons are presented between EGSnrc simulation results and experimental data of charged particle backscatter coefficients. In all graphs, the angle of incidence α (in degrees, $0 \leqslant \alpha < 90$) is the angle between the vector of the incident beam and the normal vector to the sample surface. Results for the incident electron kinetic energy of 30 keV are frequently shown only because there is a plethora of experimental data at this energy. No error bars are shown on the experimental data in the graphs for three reasons. First, the scatter among the experimental data makes enough of a statement for the purposes of this study. Second, in most experiments, only the overall uncertainties are discussed and no individual error bars are provided. Third, the systematic uncertainties discussed in section 2.1 are *not* included in the overall uncertainty reported in many of the experiments which may give a false impression about the accuracy of those experiments. For more discussion of the uncertainties associated with the experimental data, the reader is referred to section 2.1 and to the original articles of the experiments. As discussed in section 2.2, the systematic and statistical uncertainties of the EGSnrc simulations are estimated to be $\leqslant 3\%$ and $< 0.1\%$, respectively, and they are not shown for clarity of the graphs.

3.1. Electron backscatter coefficients

Figure 2 compares EGSnrc simulation results with experimental data for the variation of the electron backscatter coefficient (η_-) with the incident electron energy (E_0) for normal incidence. Low-Z samples exhibit a slight decrease in η_- as E_0 increases whereas high-Z samples exhibit the opposite trend. The EGSnrc simulation results match the average of the experimental data very well. At very low energy, the discrepancy between a number of experimental data and the EGSnrc simulation results could be partially due to the experimental uncertainties at low energy which were discussed in section 2.1, i.e. low-energy electron currents, sample contamination, detector entrance window, etc, and partially due to the EGSnrc limitations at very low energy which were discussed in section 2.2. The experimental data of Yadav and Shanker (2007) for $E_0 = 8$–28 keV and a tungsten sample are substantially lower than other experimental data and EGSnrc simulation results, and they are not included in figure 2 for graph clarity.
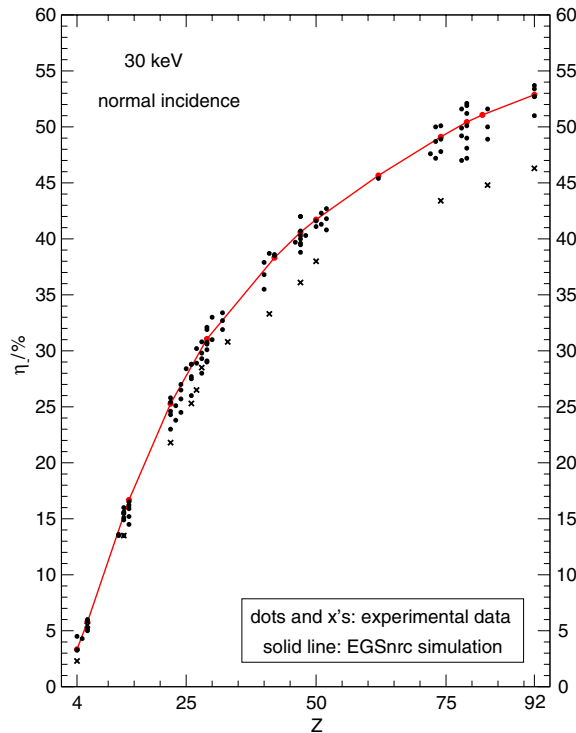
Figure 3 compares EGSnrc simulation results with experimental data for the variation of η_- with the atomic number of the sample materials (Z) for 30 keV electrons at normal incidence. The value of η_- shows a smooth and monotonic increase with Z. EGSnrc simulation results replicate this monotonic behaviour very well although they are slightly on the higher end of the scattered experimental data. The experimental data of Weinryb and Philibert (1964) ($\times$) are systematically lower than others ($\bullet$). As Bishop (1965) points out, this may be because of systematic errors introduced by the retarding grid used and by the scattering of electrons back onto the sample—both cause under-estimation of η_-.

Figure 4 compares EGSnrc simulation results with experimental data for the variation of η_- with the angle of incidence (α) in two experiments performed at two different energies with various sample materials. The value of η_- monotonically increases with α, and the increase becomes more significant as near-grazing angles are approached. This is because as α increases, the portion of the forward-peaked differential elastic scattering distribution that falls in the backscatter hemisphere increases, and thus more electrons can backscatter out of the sample, which leads to an increase in η_-. The rate of increase of η_- increases as Z decreases, which makes the variation of η_- with Z more dramatic at near-normal incidence than it is at near-grazing incidence. The EGSnrc simulation results match the two experiments very well except at near-grazing incidence on high-Z samples. This could be partially due to

Figure 2. Electron backscatter coefficient (η_-) versus incident electron kinetic energy (E_0) for normal incidence. Results are split in two panels for clarity. Experimental data are from Bishop (1965) (○), Coslett and Thomas (1965) (□), Drescher *et al* (1970) (■), Heinrich (1965) (◇), Hunger and Küchler (1979) (◆), Kulenkampff and Spyra (1954) (△), Martin *et al* (2006) (◄), Massoumi *et al* (1993) (▼), Neubert and Rogaschewski (1980) (►), Soum *et al* (1984) (+), Weinryb and Philibert (1964) (×), and Wittry (1965) (⋆). For Be and Si, Martin *et al* (2006) report two values at each energy using two different measurement techniques. Data from Kulenkampff and Spyra (1954) are at 30 keV only. The scale of the abscissa is logarithmic.
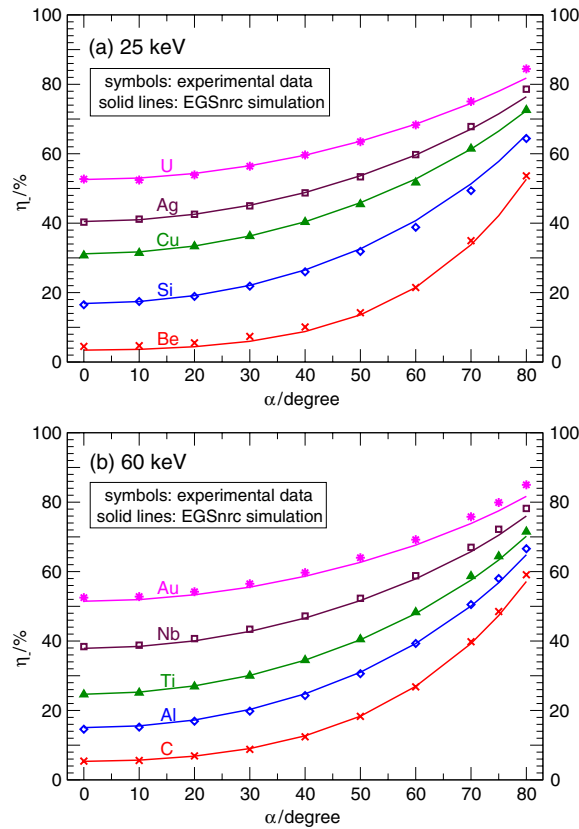
Figure 3. Electron backscatter coefficient (η_-) versus atomic number of the sample material (Z) for electrons with incident kinetic energy of 30 keV. EGSnrc simulation results are connected by solid line segments to aid the eye. Experimental data are from Bishop (1965), Drescher *et al* (1970), Heinrich (1965), Hunger and Küchler (1979), Kulenkampff and Spyra (1954), Massoumi *et al* (1993), Neubert and Rogaschewski (1980), Weinryb and Philibert (1964) and Wittry (1965). E_0 in Drescher (*et al* 1970), Hunger and Küchler (1979) and Weinryb and Philibert (1964) is not exactly 30 keV—25.2, 31.0 and 28.0 keV, respectively. Data from Weinryb and Philibert (1964) ($\times$) are systematically lower than others ($\bullet$).

the experimental uncertainties associated with near-grazing incidence which were discussed in section 2.1, i.e. incident beam masking, detector masking, sample contamination, etc, and partially due to the increased importance of electron diffraction (i.e. collective wave-like elastic scattering of electrons by the atoms of a crystalline array) at near-grazing incidence which is not modelled in EGSnrc. A slightly worse agreement (not shown) is obtained with the experimental data of Fitting and Technow (1983) for $E_0 = 10$ keV. The experimental data of Radzimski (1978) (not shown) for the variation of η_- with α for $E_0 = 10$ and 100 keV are significantly lower ($\sim$15%) than all other experimental data and EGSnrc simulation results for both normal and oblique incidence, which suggests a systematic problem with the experiment.

Before closing the discussion on electron backscatter coefficient for bulk samples, it is worth noting the difference between EGSnrc and its predecessor EGS4 (Nelson *et al* 1985) in evaluating η_-. One of the main advantages of EGSnrc over EGS4 is the improved condensed history treatment of charged particle transport (Kawrakow 2000), particularly the boundary-crossing algorithm. In a recent study of a hybrid CT/MRI system, Wen *et al* (2007b) reported that for 65 keV monoenergetic electrons normally incident on a semi-infinite tungsten target, the value of η_- evaluated using EGS4 is 54%. This is 7.4% higher than the experimental data and the EGSnrc value of 50.3% at that energy (see figure 2(b)). Although Wen *et al* (2007b)
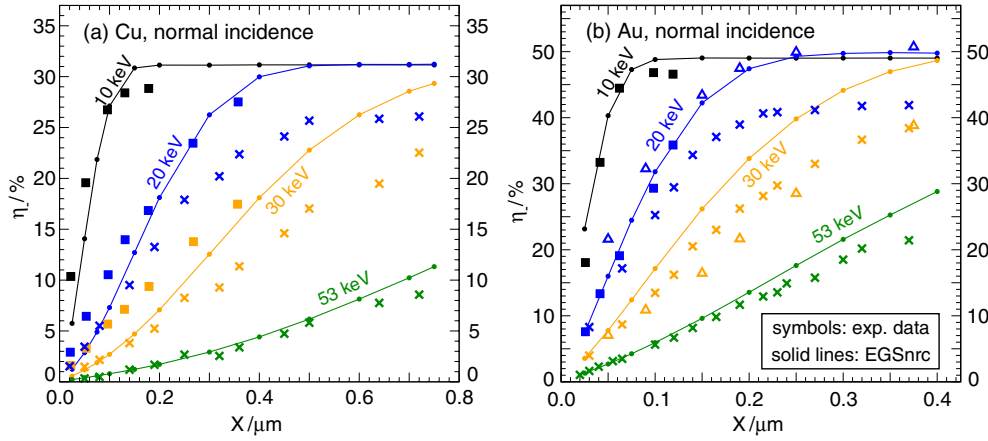
Figure 4. Electron backscatter coefficient (η_-) versus angle of incidence (α) for a 25 keV (panel a) and a 60 keV (panel b) electron beam. Simulation results are connected by solid line segments without symbols for graph clarity. Experimental data are from Drescher *et al* (1970) in panel a, and from Neubert and Rogaschewski (1980) in panel b.
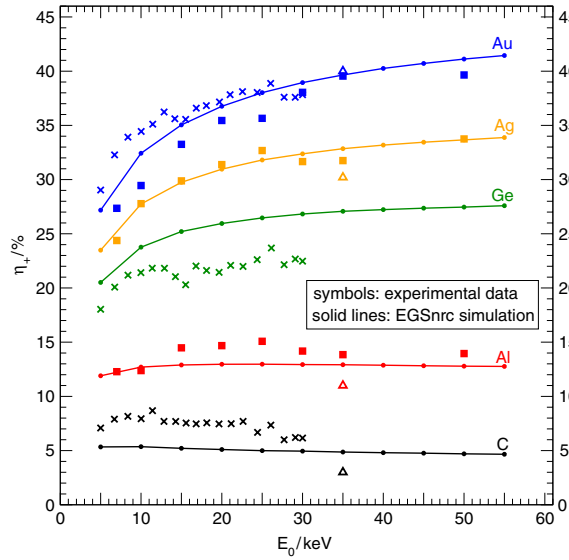
report good agreement with the experimental measurements of the x-ray tube output, better agreement would be obtained when charged particle backscatter is treated more accurately.

3.2. Backscatter from thin films

As discussed in the introduction, accurate prediction of dose perturbations due to high-Z inhomogeneities in tissue is strongly affected by the accuracy of simulating the backscatter of charged particles from thin high-Z layers (Buffa and Verhaegen 2004, Verhaegen 2002). For this reason, this section examines the capability of EGSnrc to simulate backscatter from thin films. Figure 5 compares EGSnrc simulation results with experimental data for the variation of η_- of copper and gold with film thickness for various E_0. The experiments were designed such that the thin films are self-supporting (Coslett and Thomas 1965). At small film thicknesses, the EGSnrc data for both copper and gold show an almost-linear increase of η_- with film thickness for a given incident electron kinetic energy, with the increase being steeper for lower E_0. As the film thickness increases, η_- approaches the value for bulk samples and then saturates. The saturation occurs at smaller film thicknesses for lower E_0 because the ratio of film thickness to the range of the incident electrons in the sample material increases
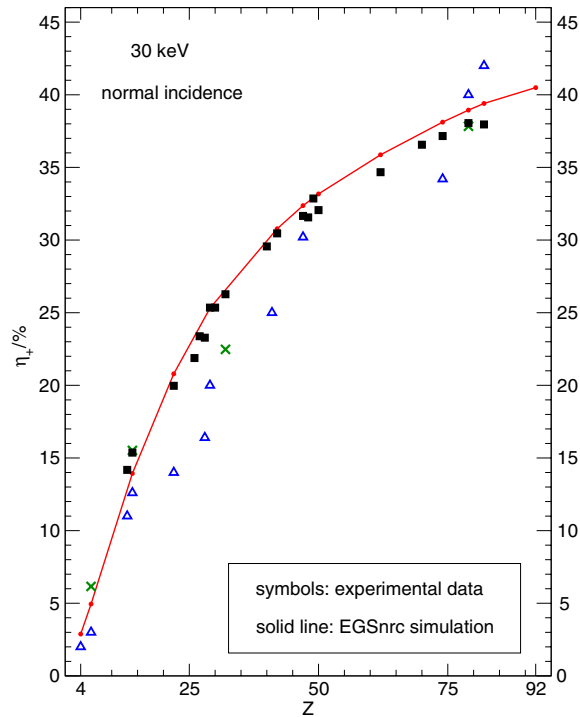
Figure 5. Backscatter from thin films: electron backscatter coefficient (η_-) versus film thickness (X) for various incident electron kinetic energies. Experimental data are from Coslett and Thomas (1965) (■), Niedrig (1982) ($\triangle$) and Niedrig and Sieber (1971) ($\times$).

Figure 6. Positron backscatter coefficient (η_+) versus incident positron kinetic energy (E_0). Experimental data are from Coleman *et al* (1992) (■), Mäkinen *et al* (1992) ($\times$) and Massoumi *et al* (1991) ($\triangle$).

as E_0 decreases. At 20 keV, the EGSnrc values of the film thickness at which η_- reaches half its saturation value, divided by the CSDA range of electrons in the sample material (from http://physics.nist.gov) are ~0.1 and ~0.07 for copper and gold, respectively. This means that about half of the backscattered electrons are backscattered from within the first 10% of their full penetration depth. The variation among the data from different experiments shown in figure 5 are more dramatic than it is for bulk materials because backscatter from thin films is fraught with more uncertainties, e.g. exact film thickness, effect of substrate material, more sensitivity to surface contamination, etc. At 20 keV for large film thicknesses, i.e.
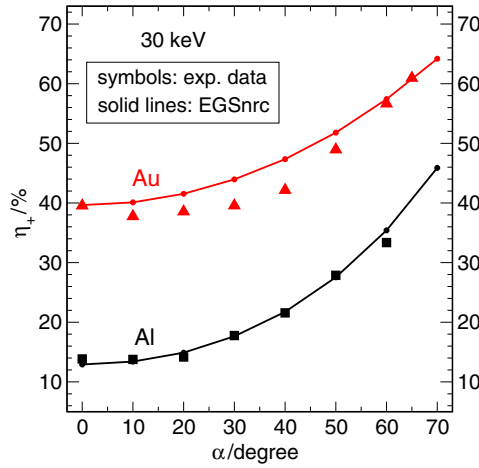
Figure 7. Positron backscatter coefficient (η_+) versus atomic number of the sample material (Z) for positrons with incident kinetic energy of 30 keV. Experimental data are from Coleman *et al* (1992) (■), Mäkinen *et al* (1992) (×) and Massoumi *et al* (1991) (△). E_0 in Massoumi *et al* (1991) is 35 keV, not 30 keV.
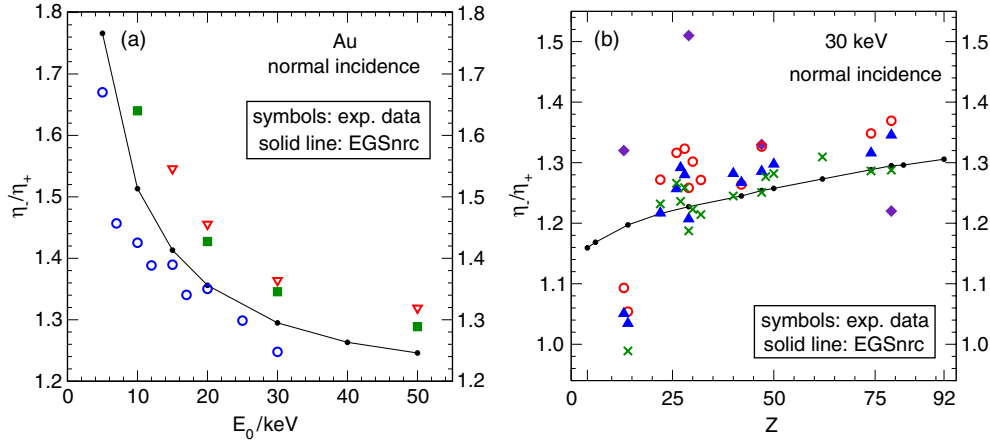
approaching bulk material behaviour, the experimental data in figure 5 saturate at η_- values (~26% and ~42% for copper and gold, respectively) much lower than those reported for bulk samples by many other experiments at the same energy (~31% and ~50% for copper and gold, respectively—see figure 2(a)). Given that experimental data for thin films are inconsistent with each other and that their saturation values are inconsistent with experimental data for bulk samples, and given that EGSnrc results reproduce the 'shapes' of the curves in figure 5 well and agree with bulk data very well (figures 2, 3 and 4), it seems reasonable to assume that EGSnrc results for backscatter from thin films are indeed accurate. More experimental work is needed to explain the inconsistency among various experiments which can then be used to better explain the discrepancies with the EGSnrc simulations.

3.3. Positron backscatter

Accurate positron transport can be important in certain positron emission tomography applications. Unlike some of the other major Monte Carlo codes, EGSnrc *always* takes into account the differences in the stopping powers and inelastic scattering cross sections between positrons and electrons (Malamut *et al* 1991). On the other hand, ETRAN-based codes (Berger and Seltzer 1973) take into account the differences between positrons and electrons only for positron beams, but not for positrons generated in pair production. This section examines the capability of EGSnrc to accurately predict η_+ in the kilovoltage range. The positron experiments included in the benchmark are only for monoenergetic positron

Figure 8. Positron backscatter coefficient (η_+) versus angle of incidence (α) of a 30 keV positron beam incident on aluminium (■) and gold (▲), respectively. Experimental data are from Coleman *et al* (1992). Experimental data at $\alpha = 65°$ are available for gold only.

Figure 9. Ratio of electron-to-positron backscatter coefficient (η_-/η_+) versus incident charged particle energy (E_0)—panel a, and versus atomic number of the sample material (Z)—panel b. In panel a, experimental ratios are: Neubert and Rogaschewski (1980)/Coleman *et al* (1992) ($\triangledown$), Massoumi *et al* (1993)/Mäkinen *et al* (1992) (○), and Heinrich (1965)/Coleman *et al* (1992) (■). In panel b, experimental ratios are: Massoumi *et al* (1991)/Massoumi *et al* (1991) (♦) (excluding the ratio of 1.75 ± 0.64 for Be, $Z = 4$—see the text), Bishop (1965)/Coleman *et al* (1992) (○), Heinrich (1965)/Coleman *et al* (1992) (▲) and Hunger and Küchler (1979)/Coleman *et al* (1992) (×). E_0 in Massoumi *et al* (1991) is 35 keV, not 30 keV.

beams. Backscatter from β^+ radioactive sources (MacKenzie *et al* 1973) is expected to yield similar agreement because it is merely a superposition of multiple monoenergetic sources. Similar to figures 2, 3 and 4 for electrons, figures 6, 7 and 8 compare EGSnrc simulation results with experimental data for the variation of η_+ with E_0, Z and α. The amount of experimental data available for positron backscatter coefficients is much less than that for electrons, and it covers a narrower energy range. The energy dependence of η_+ in figure 6 is more pronounced than that of η_- in figure 2, and EGSnrc simulation results can predict

it reasonably well. Experimental data from Mäkinen *et al* (1992) are higher than EGSnrc simulation results for a few elements and lower for others, with no particular trend. In figures 7 and 8, EGSnrc simulation results can replicate the monotonic increase of η_+ with Z and α reasonably well although the EGSnrc results are slightly on the higher end of the scattered experimental data in figure 7. Other arguments presented for electrons are also applicable to positrons.

Figure 9 compares EGSnrc simulation results with experimental data for the variation of the ratio η_-/η_+ with E_0 and Z. The experimental ratios are obtained by dividing the results from *different* electron and positron experiments. This is because, except for Massoumi *et al* (1991), no single publication has reported both electron and positron backscatter measurements. The experiments chosen to calculate η_-/η_+ are those with more complete datasets that have the same measurement parameters (Z, E_0 and α) for both electrons and positrons. Given the arbitrary nature of choosing pairs of experiments to obtain the ratio η_-/η_+ and the variation in experimental data measuring a given parameter, it can be said that EGSnrc results predict the variation of η_-/η_+ with E_0 and Z very well. For the energy range shown in figure 9(a), the ratio of electron-to-positron stopping power is $\sim$0.8 and it depends weakly on E_0 and Z (Ashley 1990). Because electrons lose less energy per unit path length, they have a higher probability of backscatter and the ratio η_-/η_+ is always >1 in that energy range. Figure 9(a) shows that the ratio increases at lower E_0 and it is $\sim$1.3 for higher E_0. This value of 1.3 has often been reported in the literature from different attempts to estimate the ratio η_-/η_+ using various experiment pairs (Coleman *et al* 1992, Massoumi *et al* 1993). Figure 9(b) shows that η_-/η_+ increases only slightly with Z. The value of η_-/η_+ from Massoumi *et al* (1991) (solid diamond) for beryllium ($Z = 4$, $\eta_-/\eta_+ = 1.75 \pm 0.64$) is not shown in figure 9(b) for clarity of other data points and also because it is reported with 40% uncertainty. The ability of EGSnrc to accurately predict η_-/η_+ is a direct result of its accounting for the differences between positron and electron transport.

4. Conclusions

This study benchmarked EGSnrc in the energy range 5–140 keV against experimental measurements of charged particle backscatter coefficients. Given the scatter in the experimental data and the excellent agreement between EGSnrc simulation results and the average of the majority of experimental data, we believe that the noted discrepancies with a few of the experiments are largely due to systematic errors in those specific experiments. At very low energies, systematic uncertainties in EGSnrc, which we estimated to be $\leqslant$3%, along with other limitations of the code could partially be the reason for a number of the discrepancies. Overall, for the energy range of interest to kilovoltage medical physics application, EGSnrc produces backscatter results within $\sim$4% of the average of the majority of published experimental data. A documented EGSnrc user-code customized for backscatter calculations is available from the authors at http://www.physics.carleton.ca/clrp/backscatter. When using BEAMnrc for kilovoltage simulations that involve component modules which use the \$BDY_TOL parameter, this study recommends using a value of \$BDY_TOL = 5×10^{-7} cm.

Acknowledgments

References

Agyingi E O, Mobit P N and Sandison G A 2005 Energy response of an aluminum oxide detector in kilovoltage and megavoltage photon beams: an EGSnrc Monte Carlo simulation study *Radiat. Prot. Dosim.* **118** 28–31

Ali E S M and Rogers D W O 2007 Efficiency improvements of x-ray simulations in EGSnrc user-codes using Bremsstrahlung cross section enhancement (BCSE) *Med. Phys.* **34** 2143–54

Ali E S M and Rogers D W O 2008a Energy spectra and angular distributions of charged particles backscattered from solid targets *J. Phys. D: Appl. Phys.* **41** 055505

Ali E S M and Rogers D W O 2008b Quantifying the effect of off-focal (extra-focal) radiation on the output of x-ray systems *Med. Phys.* submitted

Ashley J C 1990 Energy loss rate and inelastic mean free path of low-energy electrons and positrons in condensed matter *J. Electron Spectrosc.* **50** 323–34

Azner M C, Medin J, Hemdal B, King A T, Botter-Jensen L and Mattsson S 2005 A Monte Carlo study of the energy dependence of Al_2O_3:C crystals for real-time *in vivo* dosimetry *Radiat. Prot. Dosim.* **114** 444–9

Baker J A and Coleman P G 1988 Measurement of coefficients for the backscattering of 0.5–30 keV positrons from metallic surfaces *J. Phys. C: Solid State* **21** L875–80

Bazalova M and Verhaegen F 2007 Monte Carlo simulation of a computed tomography x-ray tube *Phys. Med. Biol.* **52** 5945–55

Berger M and Seltzer S 1973 ETRAN Monte Carlo code system for electron and photon transport through extended media *Report CCC-107* (Oak Ridge, TN: Oak Ridge National Laboratory (ORNL))

Berger M J and Hubbell J H 1987 XCOM: photon cross sections on a personal computer *Report NBSIR87-3597* (Gaithersburg, MD: National Institute of Standards Technology (NIST))

Bethe H A 1930 Theory of passage of swift corpuscular rays through matter *Ann. Phys.* **5** 325 (in German)

Bethe H A 1932 Scattering of electrons *Z. Phys.* **76** 293 (in German)

Bishop H E 1965 Some electron backscattering measurements for solid targets *Proc. 4th Int. Conf. on X-ray Optics and X-ray Microanalysis* ed R Castaing, P Deschamps and J Philibert (Paris: Hermann) pp 153–8

Bloch F 1933 Stopping power of atoms with several electrons *Z. Phys.* **81** 363 (in German)

Borg J, Kawrakow I, Rogers D W O and Seuntjens J P 2000 Experimental verification of EGSnrc Monte Carlo calculated ion chamber response in low-energy photon beams *Med. Phys.* **27** 1445 (abstract)

Buffa F A and Verhaegen F 2004 Backscatter and dose perturbations for low- to medium-energy electron point sources at the interface between materials with different atomic numbers *Radiat. Res.* **162** 693–701

Chow J C L, Leung M K K, Islam M K, Norrlinger B D and Jaffray D A 2008 Evaluation of the effect of patient dose from cone beam computed tomography on prostate IMRT using Monte Carlo simulation *Med. Phys.* **35** 52–60

Coleman P G, Albercht L, Jensen K O and Walker A B 1992 Positron backscattering from elemental solids *J. Phys.: Condens. Matter* **4** 10311–22

Coslett V E and Thomas R N 1965 Multiple scattering of 5–30 keV electrons in evaporated metal films: III. Backscattering and absorption *Br. J. Appl. Phys.* **16** 779–96

Deloar H *et al* 2006 Investigations of different kilovoltage x-ray energy for three-dimensional converging stereotactic radiotherapy system: Monte Carlo simulation with CT data *Med. Phys.* **33** 4635–42

Ding G X, Duggan D M and Coffey C W 2007 Characteristics of kilovoltage x-ray beams used for cone-beam computed tomography in radiation therapy *Phys. Med. Biol.* **52** 1595–615

Drescher H, Reimer L and Seidel H 1970 Backscattering and secondary electron emission of 10–100 keV and correlation to scanning electron microscopy *Z. Angew. Phys.* **29** 331–6 (in German)

Ebert M A and Carruthers B 2003 Dosimetric characteristics of a low-kV intra-operative x-ray source: implications for use in a clinical trial for treatment of low-risk breast cancer *Med. Phys.* **30** 2424–31

Fitting H J and Technow R 1983 Electron backscattering at various angles of incidence *Phys. Status Solidi* A **76** K151–4

Gérard P, Balladore J L, Martinez J P and Ouabbou A 1995 Experimental determination of angular-energy distributions of electrons backscattered by bulk gold and silicon samples *Scanning* **17** 377–86

Heinrich K F J 1965 Electron probe microanalysis by specimen current measurements *Proc. 4th Int. Conf. on X-ray Optics and X-ray Microanalysis* ed R Castaing, P Deschamps and J Philibert (Paris: Hermann) pp 159–67

Hill R, Healy B, Holloway L and Baldock C 2007 An investigation of dose changes for therapeutic kilovoltage x-ray beams with underlying lead shielding *Med. Phys.* **34** 3045–53

Hunger H J and Küchler L 1979 Measurements of the electron backscattering coefficient for quantitative EPMA in the energy range of 4 to 40 keV *Phys. Status Solidi* A **56** K45–8

ICRU 1984 Stopping powers for electrons and positrons *ICRU Report 37* (Bethesda, MD: ICRU)

Jarry G, Graham S A, Moseley D J, Jaffray D J, Siewerdsen J H and Verhaegen F 2006 Characterization of scattered radiation in kV CBCT images using Monte Carlo simulations *Med. Phys.* **33** 4320–9

Kawrakow I 2000 Accurate condensed history Monte Carlo simulation of electron transport: I. EGSnrc, the new EGS4 version *Med. Phys.* **27** 485–98

Kawrakow I and Rogers D W O 2001 The EGSnrc System, a status report *Advanced Monte Carlo for Radiation Physics, Particle Transport Simulation and Applications: Proc. Monte Carlo 2000 Meeting Lisbon* ed A Kling, F Barao, M Nakagawa, L Távora and P Vaz (Berlin: Springer) pp 135–40

Kawrakow I and Rogers D W O 2007 The EGSnrc code system: Monte Carlo simulation of electron and photon transport *NRC Technical Report PIRS-701 v4-2-2-5* (Ottawa, Canada: National Research Council of Canada) http://www.irs.inms.nrc.ca/inms/irs/EGSnrc/EGSnrc.html

Kulenkampff H and Spyra W 1954 Energy distribution of backscattered electrons *Z. Phys.* **137** 416–25 (in German)

La Russa D J, McEwen M and Rogers D W O 2007 An experimental and computational investigation of the standard temperature-pressure correction factor for ion chambers in kilovoltage x-rays *Med. Phys.* **34** 4690–9

La Russa D J and Rogers D W O 2006 An EGSnrc investigation of the P_{TP} correction factor for ion chambers in kilovoltage x-rays *Med. Phys.* **33** 4590–9

MacKenzie I K, Shulte C W, Jackman T and Campbell J L 1973 Positron transmission and scattering measurements using superposition of annihilation line shapes: backscatter coefficients *Phys. Rev.* A **7** 135–145

Mainegra-Hing E and Kawrakow I 2006 Efficient x-ray tube simulations *Med. Phys.* **33** 2683–90

Mäkinen J, Palko S, Martikainen J and Hautojärvi P 1992 Positron backscattering probabilities from solid surfaces at 2–30 keV *J. Phys.: Condens. Matter* **4** L503–8

Malamut C, Rogers D W O and Bielajew A F 1991 Calculation of water/air stopping-power ratios using EGS4 with explicit treatment of electron—positron differences *Med. Phys.* **18** 1222–8

Martin J W, Yuan J, Betancourt M J, Filippone B W, Hoedl S A, Ito T M, Plaster B and Young A R 2006 New measurements and quantitative analysis of electron backscattering in the energy range of neutron β decay *Phys. Rev.* C **73** 015501(6)

Martin J W, Yuan J, Hoedl S A, Filippone B W, Fong D, Ito T M, Lin E, Tipton B and Young A R 2003 Measurement of electron backscattering in the energy range of neutron β decay *Phys. Rev.* C **68** 055503(8)

Massoumi G R, Hozhabri N, Lennard W N and Schultz P J 1991 Doubly differential positron-backscattering yields *Phys. Rev.* B **44** 3486–89

Massoumi G R, Lennard W N and Schultz P J 1993 Electron and positron backscattering in the medium-energy range *Phys. Rev.* B **47** 11007–18

Nelson W R, Hirayama H and Rogers D W O 1985 *The EGS4 Code System Report SLAC–265* (Stanford, CA: Stanford Linear Accelerator Center)

Neubert G and Rogaschewski S 1980 Backscattering coefficient measurements of 15–60 keV electrons for solids at various angles of incidence *Phys. Status Solidi* A **59** 35–41

Niedrig H 1982 Electron backscattering from thin films *J. Appl. Phys.* **53** R15–49

Niedrig H and Sieber P 1971 Backscattering of medium/fast electrons by thin films *Z. Angew. Phys.* **31** 27–31 (in German)

Radzimski Z 1978 The backscattering of 10–120 keV electrons for various angles of incidence *Acta Phys. Pol.* A **53** 783–90

Rau E, Hoffmeister H, Sennov R and Kohl H 2002 Comparison of experimental and Monte Carlo simulated BSE spectra of multilayered structures and 'in-depth' measurements in a SEM *J. Phys. D: Appl. Phys.* **35** 1433–7

Rogers D W O, Faddegon B A, Ding G X, Ma C M, Wei J and Mackie T R 1995 BEAM: a Monte Carlo code to simulate radiotherapy treatment units *Med. Phys.* **22** 503–24

Rogers D W O, Kawrakow I, Seuntjens J P and Walters B R B 2000 NRC User Codes for EGSnrc *NRC Technical Report PIRS-702* (Ottawa, Canada: National Research Council of Canada) http://www.irs.inms.nrc.ca/inms/irs/EGSnrc/EGSnrc.html

Rogers D W O, Walters B and Kawrakow I 2007 BEAMnrc Users Manual *NRC Technical Report PIRS-509(A) rev K* (Ottawa, Canada: National Research Council of Canada) http://www.irs.inms.nrc.ca/BEAM/beamhome.html

Seltzer S M and Berger M J 1985 Bremsstrahlung spectra from electron interactions with screened atomic nuclei and orbital electrons *Nucl. Inst. Meth. Phys. Res.* B **12** 95–134

Seltzer S M and Berger M J 1986 Bremsstrahlung energy spectra from electrons with kinetic energy from 1 keV to 10 GeV incident on screened nuclei and orbital electrons of neutral atoms with $Z = 1$–100 *At. Data Nucl. Data Tables* **35** 345–418

Soum G, Ahmed H, Arnal F, Jouffrey B and Verdier P 1984 Measurement of transmission and backscatter coefficients of monoenergetic electrons (0.05–3 MeV) *J. Microsc. Spect. Elec.* **9** 1–16 (in French)

Taylor R E P, Yegin G and Rogers D W O 2006 Monte Carlo modeling of the Xoft Axxent x-ray source *Med. Phys.* **33** 2205 (abstract)

Verhaegen F 2002 Evaluation of the EGSnrc Monte Carlo code for interface dosimetry near high-Z media exposed to kilovolt and ^{60}Co photons *Phys. Med. Biol.* **47** 1691–705

Verhaegen F and Castellano I A 2002 Microdosimetric characterisation of 28 kVp MoMo RhRh RhAl WRh and MoRh mammography x-ray spectra *Radiat. Prot. Dosim.* **99** 393–6

Verhaegen F, Reniers B, Deblois F, Devic S, Seuntjens J and Hristov D 2005 Dosimetric and microdosimetric study of contrast-enhanced radiotherapy with kilovolt x-rays *Phys. Med. Biol.* **50** 3555–69

Weinryb E and Philibert J 1964 Measurement of backscatter coefficients of electrons from 5 to 30 keV *C. R. Acad. Sci., Paris* **258** 4535–8 (in French)

Wen Z, Fahrig R, Conolly S and Pelc N J 2007a Investigation of electron trajectories of an x-ray tube in magnetic fields of MR scanners *Med. Phys.* **34** 2048–58

Wen Z, Pelc N J, Nelson W R and Fahrig R 2007b Study of increased radiation when an x-ray tube is placed in a strong magnetic field *Med. Phys.* **34** 408–18

Wittry D B 1965 Secondary electron emission in the electron probe *Proc. 4th Int. Conf. on X-ray Optics and X-ray Microanalysis* ed R Castaing, P Deschamps and J Philibert (Paris: Hermann) pp 168–80

Yadav R K and Shanker R 2007 Contribution of backscattered electrons to the total electron yield produced in collisions of 8–28 keV electrons with Tungsten *Pramana-J. Phys.* **68** 507–15

Zeng G G and McCaffrey J P 2005 The response of alanine to a 150 keV x-ray beam *Rad. Phys. Chem.* **72** 537–40